# Computational Evaluation of Suspended Microcantilever and Microfluidic Channel

Iakovos Gavalas, Dimitrios I. Fotiadis, Fellow *IEEE*

***Abstract*— In this study, a static mode suspended microcantilever model was simulated employing the Finite Elements Method (FEM), to examine the deflection of the microcantilever's beam using Newtonian and Non-Newtonian fluids. The scope of this work is to design and simulate a suspended microcantilever biosensor for the determination of the fluids' dynamic viscosity and the relationship between the blood's hematocrit and the biosensor's sensitivity. These biosensors are microstructures which consist of a microfluidic channel embedded in a microcantilever biosensor. Fluid Structure Interaction (FSI) simulations performed to study the deflection of the microcantilever when Newtonian and Non-Newtonian fluids with different dynamic viscosity are used. For the dynamic viscosity determination of the Non-Newtonian fluids, the Brid-Carreau model was used. The results indicate a proportional relation between the beam's deflection and the fluids' dynamic viscosity.**

## I. Introduction

A suspended microcantilever biosensor consists of a microfluidic channel inside a microcantilever biosensor. Suspended microcantilevers have attracted the interest of the academic community since they are very sensitive, they produce minimum background electrical noise [1] and they can be integrated into small Lab-on-a-Chip (LoC) or Point- of-Care (PoC).

There are several medical applications of the microcantilevers for early stage detection of Cancer [2], Acute Myocardial Syndrome [3], Hepatitis A [4] and much more. Thus, the need of more accurate microcantilever designs is mandatory. For this reason, suspended microcantilevers have been introduced.

Burg *et al*. [5] used a suspended microcantilever resonator was used to measure the mass of biomolecules, single cells and single nanoparticles by recording the frequency shifts from the cantilever's initial resonant frequency. Among the most popular sensing methods for microcantilevers is the optical one. Its simplicity allows to be used for any type of microcantilevers. However, a major drawback is that it lacks versatility and therefore it is not suitable for Lab-on-a-Chip (LoC) solutions. To overcome this problem, various alternatives have been introduced. The capacitive method for a nanocantilever for read-out was introduced by Boisen *et al*. [6]. Faegh *et al*. used a piezoelectric cantilever to solve the sensing issue. The innovation was that the sensor could sense and actuate at the same time [7, 8]. In the same year, this idea evolved and new materials were introduced using polymers instead of silicon [9]. W.M Zhang et al. studied the Fluid Structure Interaction (FSI) between the microfluidics channel and the microcantilever beam. They have also added flowing particles [10]. A suspended microcantilever with an orthogonal flow to the bending plate of the structure, was fabricated to study the kinematic viscosity of various Newtonian and non-Newtonian fluids [11]. In the same year a simulation study of a suspended microchannel resonator nano-sensor was conducted [12]. Finite Element Methods (FEM) computations introduced for microcantilever biosensor in 2006 [13]. Marzban *et al*. used two parallel, perpendicular to microcantilever deflection direction, microfluidic channels made from polydimethylsiloxane (PDMS), to investigate the behavior of the suspended polymeric microfluidics using FSI employing FEM [14].

The innovation of our study focuses on the computational issues of a biosensor which can measure the dynamic viscosity of both Newtonian and Non-Newtonian fluid by the deflection of the microcantilever caused using fluids with different dynamic viscosities. Moreover, in this study we examined how the hematocrit of the blood affects the beam's deflection. Finally, the presented biosensor presents promising results compared to a previously published biosensor study [14] in terms of sensitivity.

## II. Materials and Methods

The flow in the Biosensor version B1 is parallel to the zx-plane and the flow is vertical to the zx-plane in version B2 (Fig. 1). The sensitivity of a microcantilever biosensor is closely related to its dimensions [15, 16] and the deflection of the beam. The more it deflects the more sensitive the biosensor is. An oblong beam with a small thickness relatively to the total length, tends to be more sensitive than other shapes.

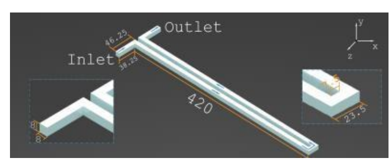


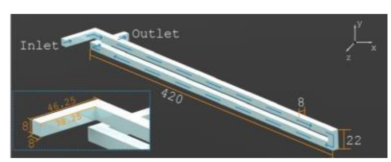


Figure 1. (Top) the microchannel domain for the Biosensor B1 and (Bottom) the microchannel domain for the Biosensor B2. The cross-section of the microchannel is 8x8 μm in both cases.

I. Gavalas is with the Department of Materials Science and Engineering, Unit of Medical Technology and Intelligent Information Systems, University of Ioannina, GR 45110, Ioannina, Greece (e-mail: igavalas@cc.uoi.gr)

D.I. Fotiadis is with the Department of Biomedical Research, Institute of Molecular Biology and Biotechnology, FORTH, Ioannina, Greece and the Dept. of Materials Science and Engineering, Unit of Medical Technology and Intelligent Information Systems, University of Ioannina, GR 45110, Ioannina, Greece (phone: +302651009006, fax: +302651008889, e-mail: fotiadis@cc.uoi.gr).

TABLE I. SOLID MATERIAL PROPERTIES

| ***Properties*** | ***PDMS*** | ***PM MA*** |
|---|---|---|
| Density (kg/m$^3$) | 0.97 | 1180 |
| Young's Modulus, E (Pa) | 3.6x10$^5$ | 2.45x |
| Poisson's Ratio | 0.49 | 0.35 |

TABLE II. FLUID PROPERTIES

| ***Fluids*** | ***Density (kg/m$^3$)*** | ***Dynamic Viscosity (Kg/ms)*** | |
|---|---|---|---|
| Blood | 1050 | 3.5x1 | |
| Water | 997 | 8.9x1 | |
| Acetone | 784 | 3.16x | |
| Propanol | 803 | 1.92x | |
| Acetic Acid | 1050 | 1.15x | |
| ***Non Newtonian Fluids*** | | High Shear Viscosity | Low Shear |
| Blood 35%H** | 1050 | 0.00313 | 0. |
| Blood 40%H** | 1050 | 0.0035 | 0. |
| Blood 48%H** | 1050 | 0.005 | 0. |
| ** As Non-Newtonian (Bird-Carreau Model) [17] | | | |

## III. NUMERICAL ANALYSIS

In order to examine the sensitivity of the two biosensors, a computational study was performed. Both the fluid flow and the fluid-structure interaction were included in the computational model. A mesh-independency analysis was performed for this study and the optimum element size was found.

### *A.* Boundary Conditions.

For both fluid domains and biosensors the boundary conditions are the same. The fluid has constant inlet velocity 0.1 mm/s and zero pressure is applied at the outlet. The no slip/no penetration conditions are also applied on the walls.The boundary conditions for the Biosensor B1 are presented in (Fig. 2). The boundary conditions are exactly the same with the B2 design. The fluid flow was considered laminar. Gravity was taken into account for the Computational Fluid Dynamics (CFD) and Mechanical Analysis.

### *B.* Mathematical Model

Using ANSYS we performed the analysis of the fluid flow and the deflection of the microcantilever's beam. The current problem dictates that a fluid flows inside the microfluidics channel and forces the beam to deflect downwards.

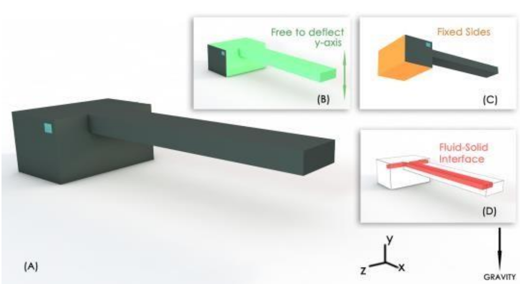


Figure 2. The boundary conditions for the biosensor B1. With green color are presented the faces which are free to deform. The orange color depicts the fixed sides of the structure, while the red color shows the fluid-structure interface.

The mechanical analysis for the deflection of the suspended microcantilever's beam was employed using the following system of equations

$$[\boldsymbol{K}]\{\boldsymbol{u}\} = \{\boldsymbol{F}\}, \tag{1}$$

where, K is the stiffness matrix of the material, u, is the nodal displacement vectors and F, is the external loads. For the CFD analysis, three components of the velocity filed $\vec{V} = v\ \hat{\imath} + v\ \hat{\jmath} + v\ \hat{k}$ and the pressure field within the $x\ \ y\ \ z$ control volume, have to be determined. Thus, using conservation principles, the mass and the momentum conservation equations are given by the Eqs. (2) and (3a, 3b and 3c), respectively. where, $\rho$ is the fluid density, $P$ is the pressure, $\mu$ is the dynamic

$$\frac{\partial \rho}{\partial t} + \frac{\partial}{\partial x}(\rho v_x) + \frac{\partial}{\partial y}(\rho v_y) + \frac{\partial}{\partial z}(\rho v_z) = 0, \tag{2}$$

$$\rho\left(\frac{\partial v_x}{\partial t} + v_x\frac{\partial v_x}{\partial x} + v_y\frac{\partial v_x}{\partial y} + v_z\frac{\partial v_x}{\partial z}\right) = -\frac{\partial P}{\partial x} - \mu\left(\frac{\partial \tau_{xx}}{\partial x} + \frac{\partial \tau_{xy}}{\partial y} + \frac{\partial \tau_{xz}}{\partial z}\right) + \rho g_x, \tag{3a}$$

$$\rho\left(\frac{\partial v_y}{\partial t} + v_x\frac{\partial v_y}{\partial x} + v_y\frac{\partial v_y}{\partial y} + v_z\frac{\partial v_y}{\partial z}\right) = -\frac{\partial P}{\partial y} - \mu\left(\frac{\partial \tau_{yx}}{\partial x} + \frac{\partial \tau_{yy}}{\partial y} + \frac{\partial \tau_{yz}}{\partial z}\right) + \rho g_y, \tag{3b}$$

$$\rho\left(\frac{\partial v_z}{\partial t} + v_x\frac{\partial v_z}{\partial x} + v_y\frac{\partial v_z}{\partial y} + v_z\frac{\partial v_z}{\partial z}\right) = -\frac{\partial P}{\partial z} - \mu\left(\frac{\partial \tau_{zx}}{\partial x} + \frac{\partial \tau_{zy}}{\partial y} + \frac{\partial \tau_{zz}}{\partial z}\right) + \rho g_z, \tag{3c}$$

fluid viscosity, $\tau$ is the stress tensor and $g$ is the earth gravity. The dynamic viscosity of a Newtonian fluid is given by:

$$\mu = \frac{\tau}{\dot{\gamma}}, \tag{4}$$

where, $\dot{\gamma}$ is the shear rate. In case of the Non-Newtonian fluid, the viscosity was calculated using the Bird- Carreau model [17]:

$$\mu = \mu_\infty + \frac{(\mu_o - \mu_\infty)}{(1 + (\lambda\dot{\gamma})^2)^{\frac{1-n}{2}}}, \tag{5}$$

where, $\mu o$ is the low shear viscosity equal to 0,056 ($Pa\ *s$), $\mu\infty$ is the high shear viscosity and it is equal to the value of the Newtonian model, $\lambda$ is a time constant equal to 3,313 s, $n$ is the power of law index equal to 0,3568 and $\dot{\gamma}$ is the shear rate. For a steady state problem as this one, the transient term $\partial\rho\ /\ \partial t$ can be neglected. For the linear elastic materials, the strain, $\boldsymbol{\varepsilon}$ and the stress, $\boldsymbol{\sigma}$ need to be determined as:

$$\boldsymbol{\sigma} = E\boldsymbol{\varepsilon}, \tag{6}$$

where, $E$ is the Young's modulus. Both the one and the two way FSI were tested. In the case of the one-way FSI, the CFD or the mechanical analysis was employed first and then, the results from the solved problem are used as initial conditions for the second one. The simulation stops when the second problem converges. For the two-way FSI, both simulations are performed at the same time by exchanging data and trying to reach an overall convergence.

## IV. RESULTS

The mechanical behavior of the biosensors with respect to the beam's deflection was tested. First, a comparison between the one and the two way FSI was performed using water, having velocity 0.1 mm/s at the inlet. The results have shown that the biosensor deflects downwards and the deflection values for the one and the two way FSI were quite close, 2.73 and 2.77 μm, respectively. Although, due to the computational time and memory requirement of the two way FSI, the one way was preferred over the two way. The Biosensor B1 exhibits larger deflections, 5.53 μm, than the B2 which deflects 0.94 μm. Thus, only the B1 version was used for the rest of the study. Two polymeric materials were tested, PDMS and PMMA. The deflection of the PDMS and PMMA was found 5.53 and 0.93 μm, respectively. The PDMS is the most suitable material since it deflects more. Three different microcantilever's beams were tested. The simulations demonstrate that the longer the beam the more it deflects. Thus, the sensitivity of the biosensor increases when the beam's length increases. As a disadvantage, the increased computational time is required as a result of the increased number of elements used in the Finite Elements (FE) calculations. Thus, the 420μm beam length was an acceptable compromise for the current study. Table III shows the beam's length, the number of the elements used in FE computations and its downwards deflection. The beam's length and the deflection are linearly related as it is shown in (Fig. 3).

Furthermore, the sensitivity of the biosensor was found to be closely related to the fluid's velocity. The higher the velocity of the fluid at the inlet, the more the biosensor deflects. A linear relationship between these two parameters was found (Fig. 4). Table IV presents the beam's deflection due to the fluid's velocity. Additionally, a linear relationship between the beam's deflection and the fluids dynamic viscosity, exists for both Newtonian and non-Newtonian fluids. The deflection of the Newtonian and Non-Newtonian fluids, with 0.1 mm/s constant inlet velocity, is presented in (Fig. 5). The velocity streamlines of the fluid flow of the B1 biosensor version, as well as the velocity field distribution in the first longest microchannel and the normalized velocity profile alongside the channel's width and height are presented in (Fig. 6). The von Mises stress was calculated and compared with the tensile strength of the material which is 2.24 MPa [18]. The resulting maximum von Mises stress, at the contact point between the biosensor's base and the beam, is 0.00267 MPa, indicating a safe structure. The very end of the tip is deflected more than the other parts of the beam, while the maximum von Mises stress appears on the opposite direction (Fig.7).

TABLE III. BEAM LENGTH VS DEFLECTION

| *Ca* | *Length (μm)* | *No. Elements* | *Deflection (μm)* |
|---|---|---|---|
| 1 | 280 | 966,972 | 0.680 |
| 2 | 420 | 1,336,553 | 5.534 |
| 3 | 630 | 6,499,618 | 13.850 |

TABLE IV. FLUID VELOCITY VS DEFLECTION

| *Case* | *Velocity (mm/s)* | *Deflection (μm)* |
|---|---|---|
| 1 | 0 (not moving) | 0.942 |
| 2 | 0.1 | 5.534 |
| 3 | 0.4 | 22.078 |
| 4 | 0.8 | 44.272 |
| 5 | 1 | 55.340 |

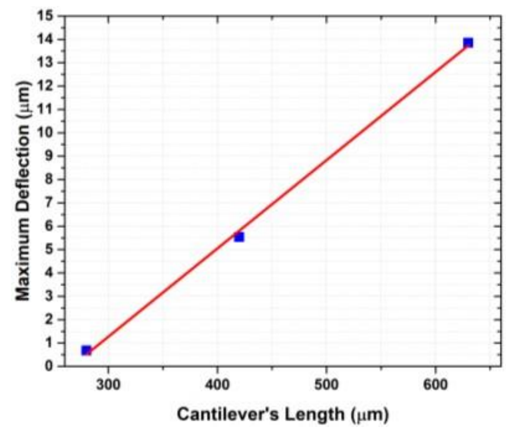


Figure 3. Maximum Deflection of the beam vs Lengths tested.

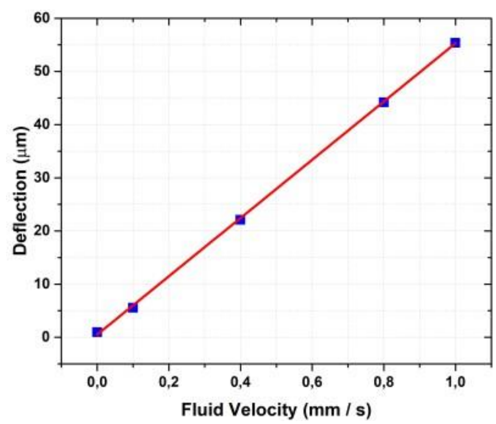


Figure 4. Maximum Deflection of the beam vs Fluid Velocity.

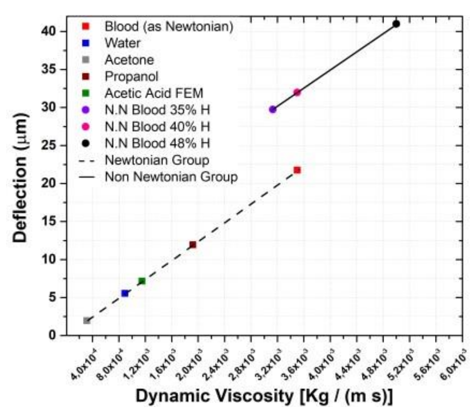


Figure 5. Maximum Deflection of the beam vs Fluid Velocity.

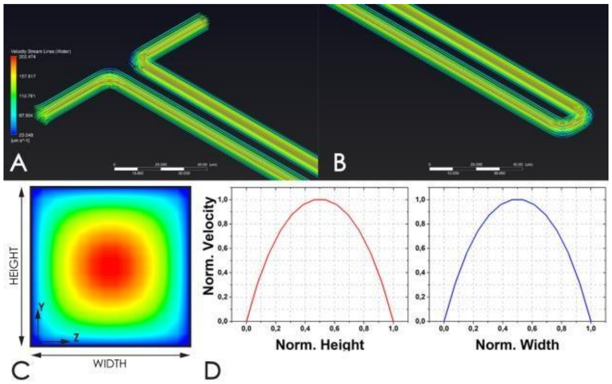


Figure 6. (A) and (B) are the velocity streamlines using water in B1 biosensor version. (C) Velocity field distribution in a cross-section inside the long microfluidics channel. (D) Normalized velocity profiles alongside the channel's height and width.

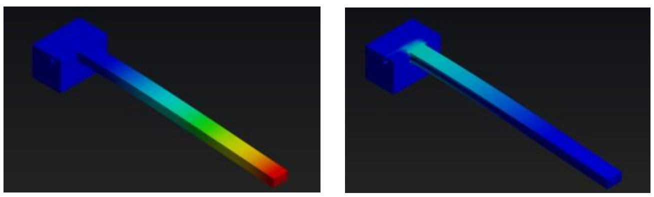

Figure 7. Areas of (Right) Maximum Deflection and (Left) Maximum von Mises Stress of the beam.

## IV. DISCUSSION AND CONCLUSIONS

The current biosensor with this small size presents unique and very promising results. The proposed biosensor B1, is able to determine the fluids' dynamic viscosity by measuring the cantilever's beam deflection with high sensitivity. The major advantage is that its encouraging results lead to a more sensitive biosensor than that proposed in the literature [14]. Fig. 8 provides a comparison of the results of this study and the literature [14] in which a bigger geometry, similar to the current B2 biosensor version, with a cantilever size of 6000 x 2000 x 600 (length, width and thickness in µm) and microfluidics cross-section of 200 x 100 µm was tested using 30 mm/s inlet velocity. By designing a significant smaller suspended microcantilever, using a geometry similar to the B1 version, better sensitivity can be achieved using lower velocities. This features set the proposed biosensor among the best candidate components for PoC or LoC devices for medical diagnostics and monitoring in terms of hematocrit measurement.

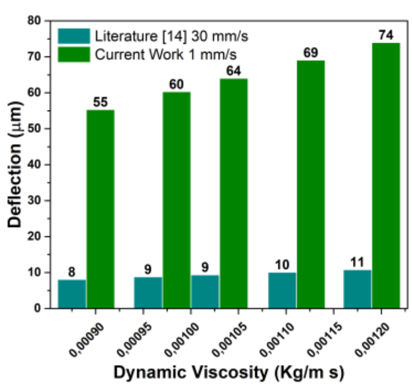


Figure 8. Comparison between the literature's data [14] and our work.

## REFERENCES


[1] Sader, John E., Thomas P. Burg, and Scott R. Manalis. "Energy dissipation in microfluidic beam resonators." *Journal of Fluid Mechanics* 650 (2010): 215-250.

[2] Chen, X., Pan, Y., Liu, H., Bai, X., Wang, N., & Zhang, B. (2016). Label-free detection of liver cancer cells by aptamer-based microcantilever biosensor. Biosensors and Bioelectronics, 79, 353- 358.

[3] Stiharu, I., Rakheja, S., & MUTHUKUMARAN PACKIRISAMY, A.
M. I. R. S. T. A. R. (2005, July). MEMS based cardiac bio-enzyme detection for the acute myocardial syndrome recognition. In Proceedings of the 9th WSEAS International Conference on Systems (pp. 1-7). World Scientific and Engineering Academy and Society (WSEAS).

[4] Timurdogan, E., Alaca, B. E., Kavakli, I. H., & Urey, H. (2011). MEMS biosensor for detection of Hepatitis A and C viruses in serum. Biosensors and Bioelectronics, 28(1), 189-194.

[5] Burg, Thomas P., *et al*. "Weighing of biomolecules, single cells and single nanoparticles in fluid." *nature 446.7139 (2007): 1066.*

[6] Boisen, Anja, *et al*. "Cantilever-like micromechanical sensors." *Reports on Progress in Physics* 74.3 (2011): 036101.

[7] Faegh, Samira, Nader Jalili, and Srinivas Sridhar. "A self-sensing piezoelectric microcantilever biosensor for detection of ultrasmall adsorbed masses: Theory and experiments." *Sensors* 13.5 (2013): 6089-6108.

[8] Faegh, Samira, *et al*. "A cost-effective self-sensing biosensor for detection of biological species at ultralow concentrations." *Journal of Applied Physics* 113.22 (2013): 224905.

[9] Nezhad, A. Sanati, *et al*. "PDMS microcantilever-based flow sensor integration for lab-on-a-chip." *IEEE Sensors journal* 13.2 (2013): 601- 609.

[10] Zhang, Wen-Ming, *et al*. "Dynamics of suspended microchannel resonators conveying opposite internal fluid flow: Stability, frequency shift and energy dissipation." *Journal of Sound and Vibration* 368 (2016): 103-120.

*[11]* Marzban, Mostapha, Muthukumaran Packirisamy, and Javad Dargahi. "3D Suspended Polymeric Microfluidics (SPMF3) with Flow Orthogonal to Bending (FOB) for Fluid Analysis through Kinematic Viscosity." *Applied Sciences 7.10 (2017): 1048.*

[12] Zakeri, Manizhe, and Seyed Mahmoud Seyedi Sahebari. "Modeling and simulation of a suspended microchannel resonator nano- sensor." Microsystem Technologies (2017): 1-14.

[13] Lee, Chia-Yen, *et al*. "Elastic–plastic modeling of heat-treated bimorph micro-cantilevers." *Microsystem Technologies* 12.10-11 (2006): 979-986.

*[14]* Marzban, Mostapha, Muthukumaran Packirisamy, and Javad Dargahi. "Parametric study on fluid structure interaction of a 3D suspended polymeric microfluidics (SPMF3)." *Microsystem Technologies* (2018): 1-11.

[15] Villanueva, G., *et al*. "Crystalline silicon cantilevers for piezoresistive detection of biomolecular forces." *Microelectronic Engineering* 85.5-6 (2008): 1120-1123.E. H. Miller, "A note on reflector arrays (Periodical style—Accepted for publication)," *IEEE Trans. Antennas Propagat.*, to be published.

[16] Lee, J., *et al*. "Suspended microchannel resonators with piezoresistive sensors." *Lab on a Chip* 11.4 (2011): 645-651.

[17] Siebert, M. W., & Fodor, P. S. (2009). Newtonian and non-newtonian blood flow over a backward-facing step–a case study. *In Proceedings of the COMSOL Conference, Boston*.

[18] Brandrup, J., Immergut, E. H., Grulke, E. A., Abe, A., & Bloch, D. R. (Eds.). (1999). Polymer handbook (Vol. 89). New York: Wiley.